

17-Jan-06

To Appear in Ecological Letters

Experimental support of the scaling rule for demographic stochasticity

**Robert A. Desharnais^{1*}, R. F. Costantino², J. M. Cushing³, Shandelle M. Henson⁴,
Brian Dennis⁵ and Aaron A. King⁶**

¹*Department of Biological Sciences, California State University, Los Angeles, CA 90032, USA*

²*Department of Ecology and Evolutionary Biology, University of Arizona, Tucson, AZ 85721, USA*

³*Department of Mathematics, University of Arizona, Tucson, AZ 85721, USA*

⁴*Department of Mathematics, Andrews University, Berrien Springs, MI 49104, USA*

⁵*Department of Fish and Wildlife resources and Division of Statistics, University of Idaho, Moscow, ID 83844, USA*

⁶*Department of Ecology & Evolutionary Biology, University of Michigan, Ann Arbor, MI 48109, USA*

**Correspondence: E-mail: rdeshar@calstatela.edu*

Running title: Scaling rule for demographic stochasticity

Type of article: Letter

There are 151 words in the abstract, 4262 words in the body, and a total of 6210 words in the manuscript. There are six figures and no tables.

Correspondence author: Robert A. Desharnais
Department of Biological Sciences
California State University, Los Angeles
5151 State University Drive
Los Angeles, CA 90032-8201
Telephone: (323) 343-2056
Fax: (323) 343-6451
E-mail: rdeshar@calstatela.edu

Abstract

A scaling rule of ecological theory, accepted but lacking experimental confirmation, is that the magnitude of fluctuations in population densities due to demographic stochasticity scales inversely with the square root of population numbers. This supposition is based on analyses of models exhibiting exponential growth or stable equilibria. Using two quantitative measures, we extend the scaling rule to situations in which population densities fluctuate due to nonlinear deterministic dynamics. These measures are applied to populations of the flour beetle *Tribolium castaneum* that display chaotic dynamics in both a 20g and 60g habitat. Populations cultured in the larger habitat exhibit a clarification of the deterministic dynamics which follows the inverse square root rule. Lattice effects, a deterministic phenomenon caused by the discrete nature of individuals, can cause deviations from the scaling rule when population numbers are small. The scaling rule is robust to the probability distribution used to model demographic variation among individuals.

Keywords

Demographic stochasticity, chaos, nonlinear population dynamics, scaling rule, habitat size, flour beetles, *Tribolium*.

INTRODUCTION

A fundamental concern in ecology is to understand how stochasticity influences the dynamics of a population. Demographic stochasticity arises from the discrete nature of organisms and the fact that individual births and deaths occur as discrete random events. Previous treatments of demographic stochasticity have focused on the variance in population density relative to the mean value for exponentially growing populations or populations with a stable deterministic equilibrium. For example, May (1974) showed that for both continuous and discrete time versions of a stochastic model with constant *per capita* birth and death rates, the mean population density grows exponentially and the coefficient of variation in population density is asymptotically proportional to $N_0^{-1/2}$, where N_0 is the initial population size. Nisbet & Gurney (1982) considered a birth-death process that is a stochastic analog of the deterministic logistic model and found that the quasi-stationary probability distribution (i.e. conditional on non-extinction) has a both a mean and variance of approximately K , where K is the carrying capacity of population numbers. Thus, the coefficient of variation of population density is approximately $K^{-1/2}$. Desharnais & Costantino (1982) analyzed a birth-death population model with a Ricker birth rate bNe^{-cN} and a mortality rate μN and found that the quasi-stationary probability distribution of population numbers has a mean of approximately $E[N] \approx c^{-1} \log(b/\mu)$ and variance of approximately $\text{Var}[N] \approx c^{-1}$ and so, as c decreases, the coefficient of variation is proportional to $E[N]^{-1/2}$. In these cases and others (Leslie 1958; Bartlett 1960; Watt 1968, Anderson *et al.* 1982; Nisbet & Gurney 1982; Costantino & Desharnais 1991), the coefficient of variation of population densities decreases according to an inverse square root rule as population numbers increase. If two populations have the same densities, but different total numbers of

individuals (which implies different habitat sizes), then density fluctuations due to demographic stochasticity will be smaller in the larger population.

These previous studies apply to single-species populations with a single age/stage class and to cases in which the deterministic version of the stochastic model has a stable equilibrium. Application of the scaling rule to populations with deterministic cyclic or aperiodic components is problematic because such populations would exhibit fluctuations in the absence of any demographic noise. Consequently, a reduction in demographic stochasticity would not necessarily result in a significant decrease in the variance of the population densities. An alternative to the examination of the variance of population densities is to consider the hypothesis that a reduction in demographic stochasticity should lead to a clarification of the deterministic dynamics; periodic or aperiodic patterns should be increasingly similar to the underlying deterministic skeleton as the overall population size increases. A procedure to quantify the clarity of the deterministic signal would allow for a study of the scaling rule in these dynamically more complex situations.

We have two goals in the present study: (1) to provide a means for extending the square root scaling rule to situations in which deterministic dynamics also contribute to population variability, and (2) to provide experimental support for the scaling rule. We introduce two measures for assessing the influence of stochasticity when a deterministic model is available for predicting changes in population densities. The first measure, d_r , is the mean length of one-time-step residual vectors. The second measure, d_s , quantifies the mean distance of the state variables to the model-predicted deterministic attractor in phase space. Since the magnitude of demographic stochasticity depends on population numbers, while the deterministic dynamics typically depend on population density, the measures d_r and d_s would be expected to decrease

in a larger habitat with the same dynamics but greater population numbers. These measures are applied to a nonlinear stochastic model for laboratory populations of the flour beetle *Tribolium castaneum* and to data from an experiment designed and conducted to test the scaling rule.

MODELS

Previous studies with the *Tribolium* experimental system (Dennis *et al.* 1995; Costantino *et al.* 1995; Dennis *et al.* 1997; Cushing *et al.* 2003) identified the following “LPA” deterministic model for the dynamics of life stage numbers:

$$\begin{aligned} L_t &= bA_{t-1} \exp\left(-\left(c_{el}/V\right)L_{t-1} - \left(c_{ea}/V\right)A_{t-1}\right), \\ P_t &= (1 - \mu_l)L_{t-1}, \\ A_t &= P_{t-1} \exp\left(-\left(c_{pa}/V\right)A_{t-1}\right) + (1 - \mu_a)A_{t-1}. \end{aligned} \tag{1}$$

Here L_t is the number of feeding larvae, P_t is the number of non-feeding larvae, pupae and callow adults, and A_t is the number of sexually mature adults at time t . The unit of time is two weeks, the approximate amount of time spent in each of the L- and P-stages. The average number of larvae recruited per adult per unit time in the absence of cannibalism is $b > 0$, and μ_l and μ_a are the larval and adult probabilities of dying in one time unit. *T. castaneum* larvae and adults eat eggs, and adults eat pupae. The exponential expressions represent the fractions of individuals surviving cannibalism in one unit of time. The cannibalism coefficients c_{el}/V , c_{ea}/V , $c_{pa}/V > 0$ are inversely related to habitat size V , which has units equal to the volume occupied by 20g of flour. In model (1), the density dynamics are invariant with respect to habitat size. However, overall numbers increase in proportion to V and therefore, in our system, the scaling rule can be expressed in terms of habitat size rather than population size.

A model of demographic stochasticity makes individual reproduction and survival probabilistic events. For *Tribolium*, we use the binomial and Poisson distributions to characterize the aggregation of demographic events within life stages (Watkins 2000; Dennis *et al.* 2001; Desharnais *et al.* 2005; Costantino *et al.* 2005). The Poisson-binomial (PB) model used in the present study is

$$\begin{aligned} L_t &\sim \text{Poisson}\left[ba_{t-1}\exp\left(-\left(c_{el}/V\right)l_{t-1}-\left(c_{ea}/V\right)a_{t-1}\right)\right], \\ P_t &\sim \text{binomial}\left[l_{t-1},\left(1-\mu_l\right)\right], \\ A_t &= \text{round}\left[p_{t-1}\exp\left(-\left(c_{pa}/V\right)a_{t-1}\right)\right] + \text{round}\left[\left(1-\mu_a\right)a_{t-1}\right], \end{aligned} \quad (2)$$

where life-stage numbers L_t and P_t are now random variables that are conditional upon the realized values l_{t-1} and a_{t-1} in the previous time step. Here, “ \sim ” means “is distributed as” and the “round” operation rounds to the nearest integer. The random variable describing the number of L-stage animals at time t is the result of a compound process: each adult produces a random number of potential recruits, which, by assumption, has a Poisson distribution with mean b , and each potential recruit subsequently undergoes an independent process of surviving cannibalism where the conditional survival probability is $\exp\left(-\left(c_{el}/V\right)l_{t-1}-\left(c_{ea}/V\right)a_{t-1}\right)$. Summing the reproductive output of all a_{t-1} adults yields a Poisson-distributed random variable for the number of L-stage animals at time t which is conditional on the expected number of individuals from the deterministic model (1). The number of pupae is described by a binomial distribution where each member of a cohort of l_{t-1} larvae is independently at risk of dying with probability μ_l . In our experiment, we manipulated adult numbers using the expression from the deterministic model (1) with the numbers of new and surviving adults confined to integer values. The number of adults in model (2) conforms to this experimental protocol. In model (2) the dynamics of life stage numbers are confined to the three-dimensional lattice of nonnegative integers.

MATERIALS AND METHODS

We experimentally evaluated the scaling rule by comparing two sets of *T. castaneum* populations with similar densities and the same deterministic dynamics, but different overall numbers. Since one of the goals of the present study is to extend the scaling rule to situations in which deterministic dynamics also contribute to population variability, we chose to focus on populations that fluctuate around a chaotic attractor. We maintained three replicate populations in 20g of flour media ($V = 1$) and a second treatment of three populations in 60g of media ($V = 3$). We subjected both sets of cultures to a laboratory protocol that fixed the adult mortality rate at $\mu_a = 0.96$ and the cannibalism rate of pupae at $c_{pa} = 0.35$ (Costantino *et al.* 1997).

Previous work has shown that these conditions produce chaotic population dynamics (Costantino *et al.* 1997; Dennis *et al.* 2001). The initial populations were composed of 250 larvae, 5 pupae and 100 adults for the 20g cultures and 114 larvae, 5 pupae and 148 adults for the 60g cultures. (The different initial stage numbers come from the fact that the 20g cultures were also part of a separate study. However, all the populations quickly approached the chaotic attractor and initial numbers were excluded from the data analyses.) All cultures were maintained in a half-pint (237 ml) milk bottles and kept in a dark incubator at 32°C. Every two weeks the larval, pupal and adult stages were counted and returned to fresh media (95% bleached wheat flour and 5% dried brewer's yeast). To control for genetic change, at every other census, adults were replaced with an equal number from the laboratory stocks. This procedure was repeated for 108 weeks yielding a time series of 54 censuses for each replicate population.

RESULTS

The L-stage densities for the six experimental populations are plotted in Fig. 1. The three populations cultured in 20g of media ($V = 1$) are on the left and the replicates for the 60g treatment ($V = 3$) are on the right. The deterministic model (1) was used with maximum likelihood parameter estimates for model (2) from a previous study (Dennis *et al.* 2001) to generate one-step predicted values for population densities. These one-step predictions are plotted as open circles in Fig. 1. Three features are worth noting. First, the overall L-stage densities in the two treatment groups are similar, lending support to the model prediction that the overall population densities scale in proportion to habitat size. Second, the one-step model predictions work well for the $V = 3$ populations, even though none of these data were used to obtain the parameter estimates. Third, the residual differences between the data points and one-step predictions are, in general, smaller for the population in the larger habitat, suggesting a decrease in the amount of demographic stochasticity.

The response of the life-stage residuals to a change in habitat size was investigated for model (2) and the experimental data. Using the parameter estimates from Dennis *et al.* (2001), the PB model was simulated 1000 times at $V = 1$ and $V = 3$ to produce two long stochastic time series. The residuals were computed as the difference between the data density values (simulated or observed) and the values predicted from the deterministic model (1) using the L-, P-, and A-stage values from the previous time step. These residuals were plotted for the PB simulations (Fig. 2a,b) and the experimental populations (Fig. 2c,d). The mean residual distance d_r was computed as the mean of the distances of residual pairs from the origin:

$$d_r = n^{-1} \sum_{t=1}^n \sqrt{\left(L_t/V - \hat{L}_t/V\right)^2 + \left(P_t/V - \hat{P}_t/V\right)^2}. \quad (3)$$

Here n is the sample size, $(L_t/V, P_t/V)$ are the data densities, and $(\hat{L}_t/V, \hat{P}_t/V)$ are the corresponding predicted values. Although the PB model tends to underestimate the magnitude of the experimental residuals, d_r decreases as V increases for both the stochastic model and the data, suggesting that a stronger deterministic signal is present when habitat size increases.

The response of the state variables to an increase in habitat size was also evaluated by looking at the data in phase space. The same stochastic realizations that were generated for the residual analysis were plotted in phase space together with the chaotic attractor predicted by the deterministic model (Fig. 3a,b). The phase space dimensions are the life-stage densities, so the number of animals is three times larger for $V=3$ compared to $V=1$. As predicted, both the PB stochastic simulations and the data scale linearly with V . In the larger habitat, the data points for both the PB simulations and the experimental populations cling more closely to the predicted chaotic attractor (Fig. 3). This was confirmed by taking each data point, finding its minimum distance in phase space from 1000 points on the deterministic attractor, and computing d_s as the mean of these minimum distances:

$$d_s = n^{-1} \sum_{t=1}^n \sqrt{\min_{i \in [1, m]} \left\{ (L_t/V - \tilde{L}_i/V)^2 + (P_t/V - \tilde{P}_i/V)^2 + (A_t/V - \tilde{A}_i/V)^2 \right\}}, \quad (4)$$

Here $\left\{ (\tilde{L}_1, \tilde{P}_1, \tilde{A}_1), (\tilde{L}_2, \tilde{P}_2, \tilde{A}_2), \dots, (\tilde{L}_m, \tilde{P}_m, \tilde{A}_m) \right\}$ is the set of m points that make up the attractor (a large finite sample of points in the case of an aperiodic attractor). The mean minimum distance d_s decreases as habitat size increases (Fig. 3).

To explore how d_r and d_s scale with V , we conducted stochastic simulations using habitat sizes from $V=1$ to $V=100$ and plotted the values of both measures on a log-log scale. For d_r , a strong linear trend with a slope of approximately -0.5 is evident throughout most of

the range of habitat sizes, except for slight deviations near $V = 1$ (Fig. 4a). This indicates an inverse square root scaling of the residuals as habitat size increases. For d_s , a strong linear trend with a slope of approximately -0.5 exists for $V > 5$, but significant departures are present for smaller habitat sizes (Fig. 4b). These deviations are the result of “lattice effects” which were documented in previous studies (Henson *et al.* 2001, King *et al.* 2004, Scheuring & Domokos 2005). Confining the deterministic dynamics of animal numbers to integer values leads to cyclic attractors that may differ significantly from the continuous-model attractors. When $V = 1$ there is a strong lattice cycle with period of six as well as other weaker lattice cycles with periods of eight and three (King *et al.* 2004). One can see evidence of this 6-cycle in the phase space plots as aggregations of points for the simulations (Fig. 3a) and the experimental data (Fig. 3c) that are far from the chaotic attractor. For example, the clusters of data points located above and to the right side of the chaotic attractor along the A-stage axis are near two of the fixed points of the period six lattice cycle (Fig. 3a,c). The mean minimum distance of the predicted lattice 6-cycle from the continuous attractor is 24.1 which is close to the maximum d_s value obtained for the PB simulations at $V=1$ (Fig. 4b).

A study of the ratios of the d_r and d_s measures for the two habitat volumes provides experimental support for the inverse square root scaling rule (Fig. 5). We obtained sampling distributions for these ratios from the PB model (2) using the experimental protocol, and for comparison, we calculated d_r and d_s ratios in the same way for all nine possible pairings of the three experimental replicates for $V = 3$ and $V = 1$. (These ratios are not independent estimates, since each replicate is used in three of the ratios.) Since the replicates at $V = 3$ have numbers that are, on average, three times larger than replicates at $V = 1$, the expected ratio for this rule is $\sqrt{1/3} \approx 0.577$. The experimental d_r ratios scatter around this value and are mostly contained

within a predicted 95% confidence interval based on PB model simulations (Fig. 5a). For the d_s ratios, the observed values fall within the long right tail of the predicted distribution (Fig. 5b). Because the d_s values at $V = 1$ are inflated due to an accumulation of points around lattice cycles, the majority of the simulated ratios fall below the predicted 0.577. When the volumes increase by a factor of ten, the influence of lattice cycles diminishes (Fig. 5c,d).

ROBUSTNESS OF THE SCALING RULE

Although the inverse square root scaling rule has been demonstrated for a variety of stochastic models (Kendall 1949; Bartlett 1960; May 1973; Nisbet & Gurney 1982), its generality remains an open question. In the present study one could be misled into believing that the scaling rule is a consequence of our choice of the Poisson distribution in model (2) to represent variation among individuals in the production of potential recruits. For a Poisson random variable X , the mean $E(X)$ and variance $\text{Var}(X)$ are equal, and so the coefficient of variation is $\text{CV}(X) = \sqrt{\text{Var}(X)}/E(X) = 1/\sqrt{E(X)}$. This suggests inverse square root scaling. However, for demographic stochasticity, the inverse square root scaling arises through a process that is not tied to the Poisson distribution.

As an example, consider the equation for larval numbers. Let X_i be a random variable for the number of larvae produced by adult i in the absence of cannibalism. Assume $E(X_i) = b$ and $\text{Var}(X_i) = \sigma^2$. Let Y_{it} be the total number of larvae produced by adult i that survive cannibalism from time t to time $t+1$. The random variable Y_{it} will be a random sum of X_i independent Bernoulli random variables, each with a probability $\phi_t = \exp(-c_{el}l_t/V - c_{ea}a_t/V)$ of survival. From the rules for conditional expectations (e.g. Minh 2001), one can show that

$E(Y_{it}) = b\phi_t$ and $\text{Var}(Y_{it}) = b\phi_t(1-\phi_t) + \sigma^2\phi_t^2$. The total number of L-stage insects at time $t+1$

will be a random variable given by $L_{t+1} = \sum_{i=1}^{a_t} Y_{it}$, where a_t is the number of adults at time t . If we

assume the fecundity and survival events are independent, the mean and variance of this random variable will be $E(L_{t+1}) = a_t E(Y_{it})$ and $\text{Var}(L_{t+1}) = a_t \text{Var}(Y_{it})$. The coefficient of variation of

L_{t+1} is

$$\text{CV}(L_{t+1}) = \frac{\sqrt{\text{Var}(L_{t+1})}}{E(L_{t+1})} = \frac{\sqrt{a_t \text{Var}(Y_{it})}}{a_t E(Y_{it})} = \frac{\sqrt{b\phi_t(1-\phi_t) + \sigma^2\phi_t^2}}{b\phi_t\sqrt{a_t}}. \quad (5)$$

If population numbers scale with habitat size, then l_t and a_t will be proportional to V . This means that ϕ_t will not change with V and so the coefficient of variation for the residuals of L-stage numbers (5) will follow the inverse square root rule. Since a coefficient of variation is invariant to a linear transformation of the random variable, the residuals in L-stage densities will also follow the inverse square root rule. This is true for any arbitrary probability distribution for *per capita* fecundity X_i that has a positive mean and finite variance; it does not rely on the Poisson distribution.

To illustrate, we considered a stochastic LPA model that uses a negative binomial distribution in place of the Poisson for the *per capita* fecundity X_i , with $E(X_i) = b$ and $\text{Var}(X_i) = \sigma^2$. The P-stage and A-stage equations were the same as in model (2). Using the same parameter values that were used for the PB model, we conducted simulations with habitat sizes from $V = 1$ to $V = 100$ and two different variances of the random variable X_i : $\sigma^2 = 5b$ and $\sigma^2 = 10b$. (For the Poisson model, $\sigma^2 = b$.) We plotted the values of d_r and d_s versus V on a

log-log scale. Outside the range of influence of lattice effects, the inverse square root scaling rule holds for this negative binomial version of the stochastic LPA model (Fig. 6).

DISCUSSION

Previous studies of demographic stochasticity focused on the how the variance in population densities changes as population size increases. Implicit was the assumption that all fluctuations in population numbers are due to random demographic events. This precluded the possibility of nonlinear dynamics as a source of population variability. In the present study we take the perspective that population fluctuations are the joint result of deterministic forces and demographic stochasticity. By looking at the clarity of the deterministic signal in both the time series and in phase space, we were able to extend the analysis to situations where population densities cycle or have aperiodic behavior such as invariant loops and chaos. A valid mechanistic model of the deterministic sources of population variability is a prerequisite for the use of the measures d_r and d_s proposed here to evaluate the effects of demographic noise. Finding such models for natural systems is a continuing challenge (Kendall *et al.* 1999; Turchin 2003).

There is an increasing awareness of the importance of transient dynamical behavior in ecological systems (Hastings 2004). Populations may take a long time to approach their asymptotic behavior. Also, unstable invariant sets with stable manifolds (“saddles”) may exert their influence in the presence of stochasticity. For example, Cushing *et al.* (1998) provide experimental evidence for “flybys” of a saddle equilibrium in *Tribolium* populations with a stable two-cycle attractor and King *et al.* (2004) present evidence of flybys of longer-period saddle cycles in chaotic *Tribolium* population data. In the present study, d_s measures the mean minimum distance of population densities from its asymptotic attractor and would be

inappropriate when transient behavior dominated the population time series. On the other hand, the mean residual distance, d_r , is based on deviations of the population densities from their predicted values for one time step. Since transients are a model-predicted behavior, d_r could be used in these situations to evaluate the influence of demographic stochasticity.

Demographic stochasticity and lattice effects both occur when population numbers are small. The present study illustrates the difference between these two phenomena. Demographic stochasticity is a *random* phenomenon that arises from the fact that individual births and deaths occur as discrete probabilistic events. At small population sizes this can be a significant source of variation in population densities. For example, if each of ten individuals in a population has a 50% chance of surviving to the next census and the survival outcome of each individual is an independent event, then the expected coefficient of variation in the number of survivors is 0.316. On the other hand, if there are 1000 individuals, the coefficient of variation is only 0.0316. Thus, a 100-fold increase in population numbers result in a ten fold decrease in the relative magnitude of the fluctuations in the number of survivors—a simple example of the inverse square root scaling rule. Lattice effects are a *deterministic* phenomenon that occurs because, when habitat size is small, state space is discretized onto a lattice of possible population densities. If population size is bounded, deterministic dynamics on this lattice lead to periodic cycles (Henson *et al.* 2001; Henson *et al.* 2003). For example, a continuous-state chaotic attractor may be broken into multiple asymptotic cycles with patchy basins of attraction. Deterministic dynamics are cyclic (not chaotic), with periods depending on initial conditions. Stochasticity acting on small discrete-valued populations allows populations to move from one basin of attraction to another visiting each of the cycles (King *et al.* 2004). However, depending on habitat size, the dominant lattice cycles can differ significantly from the predicted continuous attractor in state space. The

mean state space distance measure, d_s , reveals these lattice effects as large deviations from the predicted inverse square root rule (Fig. 4b, Fig. 6b,d) because the demographic stochasticity is causing deviations from the deterministic lattice attractors rather than the continuous state space attractor and these lattice attractors are far from the continuous attractor when habitat size is small. As habitat size increases, the lattice of possible population densities becomes more finely spaced and the cyclic lattice attractors will lie closer to the continuous attractor in state space, although this convergence may not happen in a simple monotonic fashion (Henson *et al.* 2001). Thus, the state space distance measure d_s may serve as a useful tool for predicting the relative contributions of demographic stochasticity and lattice effects on population dynamics.

Our choice of the Poisson distribution in model (2) to describe the random variation among individuals in the number of offspring produced per adult was based on both convenience and the fact that it has been used in previous studies involving *Tribolium* and the LPA model (Watkins 2000; Dennis *et al.* 2001; Desharnais *et al.* 2005; Costantino *et al.* 2005). One of the advantages of the Poisson is that no new parameters are introduced; the deterministic and stochastic models have the same seven parameters. This allowed us to use previous parameter estimates for the LPA model (Dennis *et al.* 2001). (The habitat size parameter V is determined by the experimental protocol.) However, it is evident from the residuals (Fig. 2) that the Poisson underestimates the magnitude of variation in life stage densities. There are several possible reasons for this. The Poisson distribution does not take into account fluctuations in the number of males and females among adults which could be an important source of variability when adult numbers are small. The Poisson distribution also assumes that adults are identical with respect to their expected contribution of offspring, b . One model that relaxes this assumption is to assume that the parameter b itself has an underlying gamma probability distribution. This compound

distribution leads to a negative binomial probability model for the number of offspring produced per adult prior to cannibalism. As discussed in the previous section, the inverse square root scaling rule for demographic stochasticity is robust to the choice of the probability distribution used for adult fecundity (Fig. 6). The inadequacy of the Poisson model underscores the point made by Clark (2003) that intrinsic differences among individuals should receive greater attention as a source of variability in studies of population dynamics.

Experimental support for the scaling rule has implications for a variety of population systems, from conservation studies and population viability analyses (Schaffer 1981; Beissinger & McCullough 2002; Morris & Doak 2002), to epidemiological studies where there is an increasing appreciation for the role of demographic stochasticity (Bjørnstad *et al.* 2002; Grenfell *et al.* 2002; Lloyd 2004). However, additional factors may need to be considered when applying the findings of the present study to other systems. Here the populations are assumed to be “well mixed” so that interactions among individuals depend on global densities. In large natural populations, interactions among individuals may have a spatial component, which could have implications for the relative effects of demographic stochasticity as habitat sizes increase, especially if the habitat is heterogeneous. External sources of variability (environmental stochasticity) that affect all individuals simultaneously, such as weather, may also cause fluctuations in population densities (Athreya & Karlin 1971; May 1973). In general, demographic and environmental stochasticity will act in concert to cause deviations from deterministic dynamical predictions (Lande 1993; Engen *et al.* 1998; Sæther 2000; Vucetich & Peterson 2004). However, even in these situations, the demographic component of the noise should decrease as population numbers increase.

The original interpretation of the scaling rule for populations exhibiting exponential growth or stable equilibria was that when population numbers are sufficiently large demographic stochasticity can be ignored (Leslie 1958; May 1973; Maynard-Smith 1974). The scaling rule has been demonstrated for a variety of models (Bartlett 1960; Watt 1968, Anderson *et al.* 1982; Nisbet & Gurney 1982; Costantino & Desharnais 1991) and it is likely that it can be justified on very general grounds, although we are unaware of any theoretical treatment that shows this to be true. The scaling rule is often presented as a justification for the use of deterministic models. However, prior to the present study, we were unaware of any experimental studies that directly tested the inverse square root scaling rule. This assumption, often cited as an ecological principle, now has a firmer empirical footing.

ACKNOWLEDGEMENTS

This research was supported, in part, by grants from the U.S. National Science Foundation (DMS 9973126, DMS 9981374, DMS 9981423, DMS 9981458, DMS 0443803).

REFERENCES

- Anderson, R. M., Gordon, D. M., Crawley, M. J. & Hassell, M. P. (1982). Variability in the abundance of animal and plant species. *Nature*, 296, 245–248.
- Athreya, K. B. & Karlin, S. (1971). On branching processes with random environments. I. Extinction probabilities. *Ann. Math. Stat.*, 42, 1499–1520.
- Bartlett, M. S. (1960). *Stochastic Population Models*. London, Methuen.
- Beissinger, S. R. & McCullough, D. R. (2002). *Population Viability Analysis*. Univ. of Chicago Press, Chicago, IL.

- Bjørnstad, O. N., Finkenstädt, B. F. & Grenfell, B. T. (2002). Dynamics of measles epidemics: estimating scaling of transmission rates using a time series SIR model. *Ecol. Monogr.*, 72, 169–184.
- Clark, J. S. (2003). Uncertainty and variability in demography and population growth: a hierarchical approach. *Ecology*, 84, 1370–1381.
- Costantino, R. F. & Desharnais, R. A. (1991). *Population Dynamics and the Tribolium Model: Genetics and Demography*. Springer-Verlag, New York, NY.
- Costantino, R. F., Cushing, J. M., Dennis, B. & Desharnais, R. A. (1995). Experimentally induced transitions in the dynamic behavior of insect populations. *Nature*, 375, 227–230.
- Costantino, R. F., Desharnais, R. A., Cushing, J. M. & Dennis, B. (1997). Chaotic dynamics in an insect population. *Science*, 275, 389–391.
- Costantino, R. F., Desharnais, R. A., Cushing, J. M., Dennis, B., Henson, S. M. & King A. A. (2005). Nonlinear stochastic population dynamics: The flour beetle *Tribolium* as an effective tool of discovery. In: *Population Dynamics and Laboratory Ecology* (ed. Desharnais, R. A.). Academic Press, New York, NY.
- Cushing, J. M., Dennis, B., Desharnais, R. A. & Costantino, R. F. (1998). Moving toward an unstable equilibrium: saddle nodes in population systems. *J. Anim. Ecol.*, 67: 298–306.
- Cushing, J. M., Costantino, R. F., Dennis, B., Desharnais, R. A. & Henson, S. M. (2003). *Chaos in Ecology: Experimental Nonlinear Dynamics*. Academic Press, New York, NY.
- Dennis, B., Desharnais, R. A., Cushing, J. M. & Costantino, R. F. (1995). Nonlinear demographic dynamics: mathematical models, statistical methods, and biological experiments. *Ecol. Monogr.*, 65, 261–281.

- Dennis, B., Desharnais, R. A., Cushing, J. M. & Costantino, R. F. (1997). Transitions in population dynamics: equilibria to periodic cycles to aperiodic cycles. *J. Anim. Ecol.*, 66, 704–729.
- Dennis, B., Desharnais, R. A., Cushing, J. M., Henson, S. M. & Costantino, R. F. (2001). Estimating chaos and complex dynamics in an insect population. *Ecol. Monogr.*, 71, 277–303.
- Desharnais, R. A. & Costantino, R. F. (1982). The approach to equilibrium and the steady-state probability distribution of adult numbers in *Tribolium brevicornis*. *Am. Nat.* 119, 102–111.
- Desharnais, R. A., Edmunds, J., Costantino, R. F. & Henson, S. M. (2005). Species competition: uncertainty on a double invariant loop. *J. Difference Equ. Appl.*, 11, 311–325.
- Engen, S., Bakke, Ø. & Islam, A. (1998). Demographic and environmental stochasticity—concepts and definitions. *Biometrics*, 54, 840–846.
- Grenfell, B. T., Bjørnstad, O. N. & Finkenstädt, B. F. (2002). Dynamics of measles epidemics: scaling noise, determinism, and predictability with the TSIR model. *Ecol. Monogr.*, 72, 185–202.
- Hastings, A. (2004). Transients: the key to long-term ecological understanding? *Trends Ecol. Evolut.*, 29, 39–45.
- Henson, S. M., Costantino, R. F., Cushing, J. M., Desharnais, R. A., Dennis, B. & King A. A. (2001). Lattice effects observed in chaotic dynamics of experimental populations. *Science*, 294, 602–605.

- Henson, S. M., King, A. A., Costantino, R. F., Cushing, J. M., Dennis, D. & Desharnais, R. A. (2003). Explaining and predicting patterns in stochastic population systems. *Proc. Roy. Soc. London B*, 270, 1549–1553.
- Kendall, B. E., Briggs, C. J., Murdoch, W. W., Turchin, P., Ellner, S. P., McCauley, E., Nisbet, R. M. & Wood, S. N. (1999). Why do populations cycle? A synthesis of statistical and mechanistic modeling approaches. *Ecology*, 80, 1789–1805.
- Kendall, D. G. (1949). Stochastic processes and population growth. *J. Roy. Stat. Soc., B*, 11, 230–264.
- King, A. A., Costantino, R. F., Cushing, J. M., Henson, S. H., Desharnais, R. A. & Dennis, B. (2004). Anatomy of a chaotic attractor: Subtle model-predicted patterns revealed in population data. *Proc. Natl. Acad. Sci. USA*, 101, 408–413.
- Lande, R. (1993). Risks of population extinction from demographic and environmental stochasticity and random catastrophes. *Am. Nat.*, 142, 911–927.
- Leslie, P. H. (1958). A stochastic model for studying the properties of certain biological systems by numerical methods. *Biometrika*, 45, 16–31.
- Lloyd, A. L. (2004). Estimating variability in models for recurrent epidemics: assessing the use of moment closure techniques. *Theor. Popul. Biol.*, 65, 49–65.
- May, R. M. (1973). *Stability and Complexity in Model Ecosystems*. Princeton Univ. Press, Princeton, NJ.
- Maynard Smith, J. (1974). *Models in Ecology*. Cambridge Univ. Press, Cambridge, UK.
- Minh, D. L. (2001). *Applied Probability Models*. Duxbury, Pacific Grove, CA.
- Morris, W. F. & Doak, D. F. (2002). *Quantitative Conservation Biology: Theory and Practice of Population Viability Analysis*. Sinauer Associates, Sunderland, MA.

- Nisbet, R. M. & Gurney, W. S. C. (1982). *Modelling Fluctuating Populations*. John Wiley & Sons, New York, NY.
- Sæther, B.-E. Tufto, J., Engen, S., Jerstad, K., Røstad, O. W. & Skåtan, J. E. (2000). Population dynamical consequences of climate change for a small temperate songbird. *Science*, 287, 854–856.
- Scheuring, I. & Domokos, G. (2005). Sturdy cycles in the chaotic *Tribolium castaneum* data series. *Theor. Popul. Biol.*, 67, 127–139.
- Shaffer, M. L. (1981). Minimum population sizes for species conservation. *Bioscience*, 31, 131–134.
- Turchin P. (2003). *Complex Population Dynamics: a Theoretical/Empirical Synthesis*. Princeton University Press, Princeton, NJ.
- Vucetich, J. A. & Peterson, R. O. (2004). The influence of prey consumption and demographic stochasticity on population growth rate of Isle Royale wolves *Canis lupus*. *Oikos*, 107, 309–320.
- Watkins, J. C. (2000). Consistency and fluctuation theorems for discrete time structured population models having demographic stochasticity. *J. Math. Biol.*, 41, 253–271.
- Watt, K. E. F. (1968). *Ecology and Resource Management: A Quantitative Approach*. McGraw-Hill, New York, NY.

FIGURE LEGENDS

Figure 1 Time series of L-stage densities for the six experimental populations. Closed circles are the observed densities and open circles are the one-step predictions for the deterministic model (1) with parameter values $b = 10.67$, $c_{el} = 0.01647$, $c_{ea} = 0.01313$, $c_{pa} = 0.35$, $\mu_l = 0.1955$, and $\mu_a = 0.96$. On the left are the populations cultured in 20g of media ($V = 1$); on the right are the populations cultured in 60g of media ($V = 3$).

Figure 2 Predicted and observed one-step residuals for the L- and P-stages. In (a) and (b) the residuals are the results for 1000 iterations of the PB-model (2) with parameter values from Fig. 1 and (a) $V = 1$ or (b) $V = 3$. In (c) and (d) are the residuals for the experimental observations. The mean distances d_r of the residuals from the origin are given in each panel.

Figure 3 Phase space plots of the PB-model simulations and the experimental data. In (a) and (b) are the same PB-model simulations that appear in Fig. 2. In (c) and (d) are the data from the three replicate populations in the two experimental treatments with the initial condition omitted. Open circles are the stochastic simulations or experimental data and closed circles are 1000 points on the chaotic attractor. The mean minimum distance d_s of the state variables from the chaotic attractor is listed in each panel.

Figure 4 Scaling of distance measures d_r and d_s with habitat volume. Values from $V = 1$ to $V = 100$ were chosen on the logarithmic scale. For each V , the PB-model was iterated 100 times to eliminate transients and then 1000 times to compute (a) d_r and (b) d_s . A linear regression from

$V = 2$ to $V = 100$ yielded the equation listed in (a). A linear regression from $V = 5$ to $V = 100$ yielded the equation listed in (b). In (b) lattice effects caused deviations for $V < 5$.

Figure 5 Distribution of d_r and d_s ratios for different habitat volumes. The PB-model was used to simulate a pair of replicates with $V = 1$ and $V = 3$ using the experimental protocol. The distance measures were computed for each replicate pair as was the ratio of the measures for $V = 3$ to $V = 1$. This was repeated 10,000 times and the sampling distributions of the d_r ratios (a) and d_s ratios (b) were estimated as histograms. The distributions in (c) and (d) were obtained in the same way for $V = 10$ and $V = 30$. The solid vertical lines are the theoretical expectation of $\sqrt{1/3} \approx 0.577$ and the dashed vertical lines are 95% confidence intervals. The arrows in (a) and (b) are all possible $V = 1$ to $V = 3$ ratios for the experimental populations.

Figure 6 Scaling of distance measures d_r and d_s with habitat volume for a stochastic LPA model with a negative binomial *per capita* fecundity distribution. Values from $V = 1$ to $V = 100$ were chosen on the logarithmic scale. For each V , the stochastic model was iterated 100 times to eliminate transients and then 1000 times to compute (a, c) d_r and (b, d) d_s . In panels (a) and (b), the negative binomial distribution has a variance equal to five times the mean. In panels (c) and (d), the negative binomial distribution has a variance equal to ten times the mean. A linear regression from $V = 2$ to $V = 100$ yielded the equations listed in (a) and (c). A linear regression from $V = 5$ to $V = 100$ yielded the equations listed in (b) and (d).

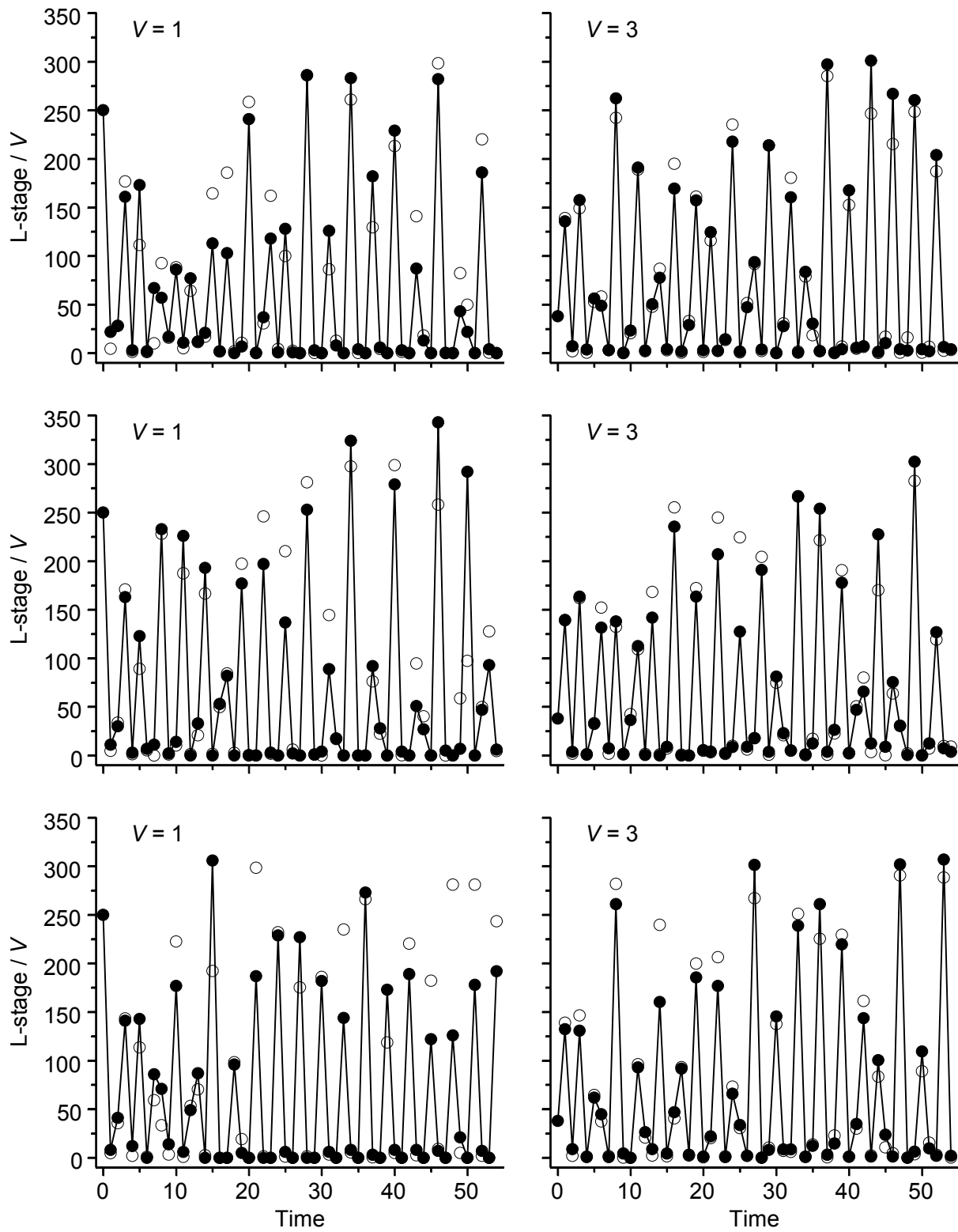


Figure 1

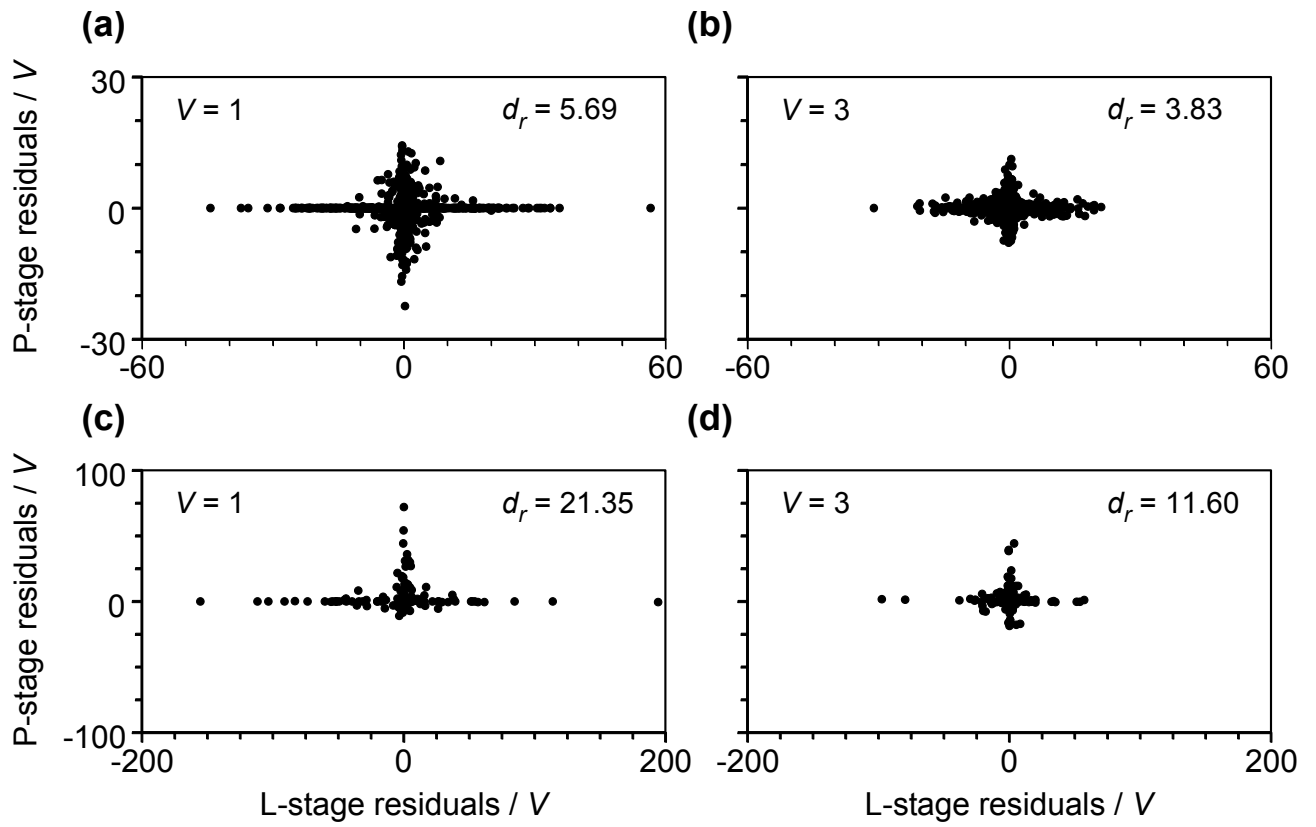


Figure 2

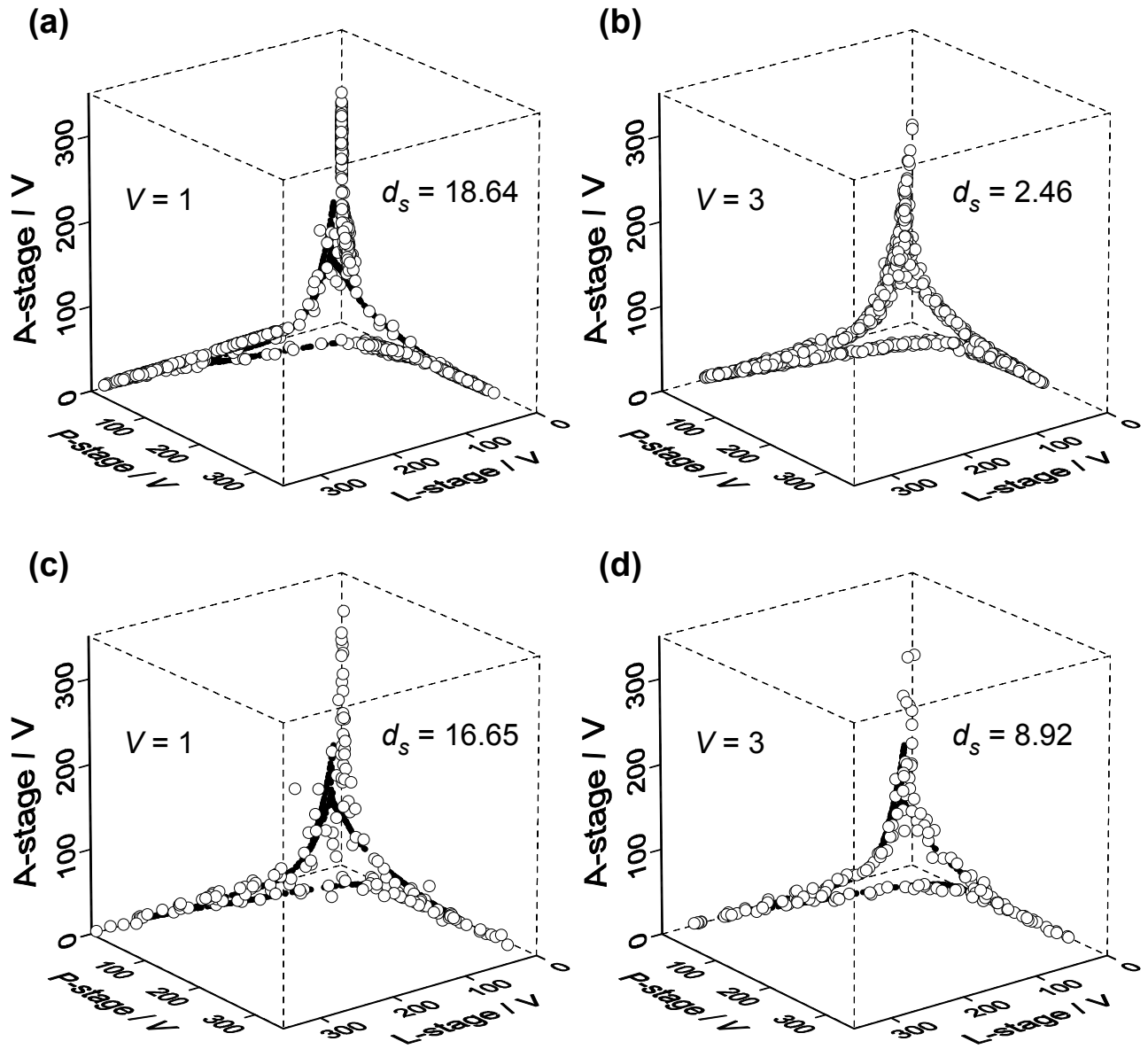


Figure 3

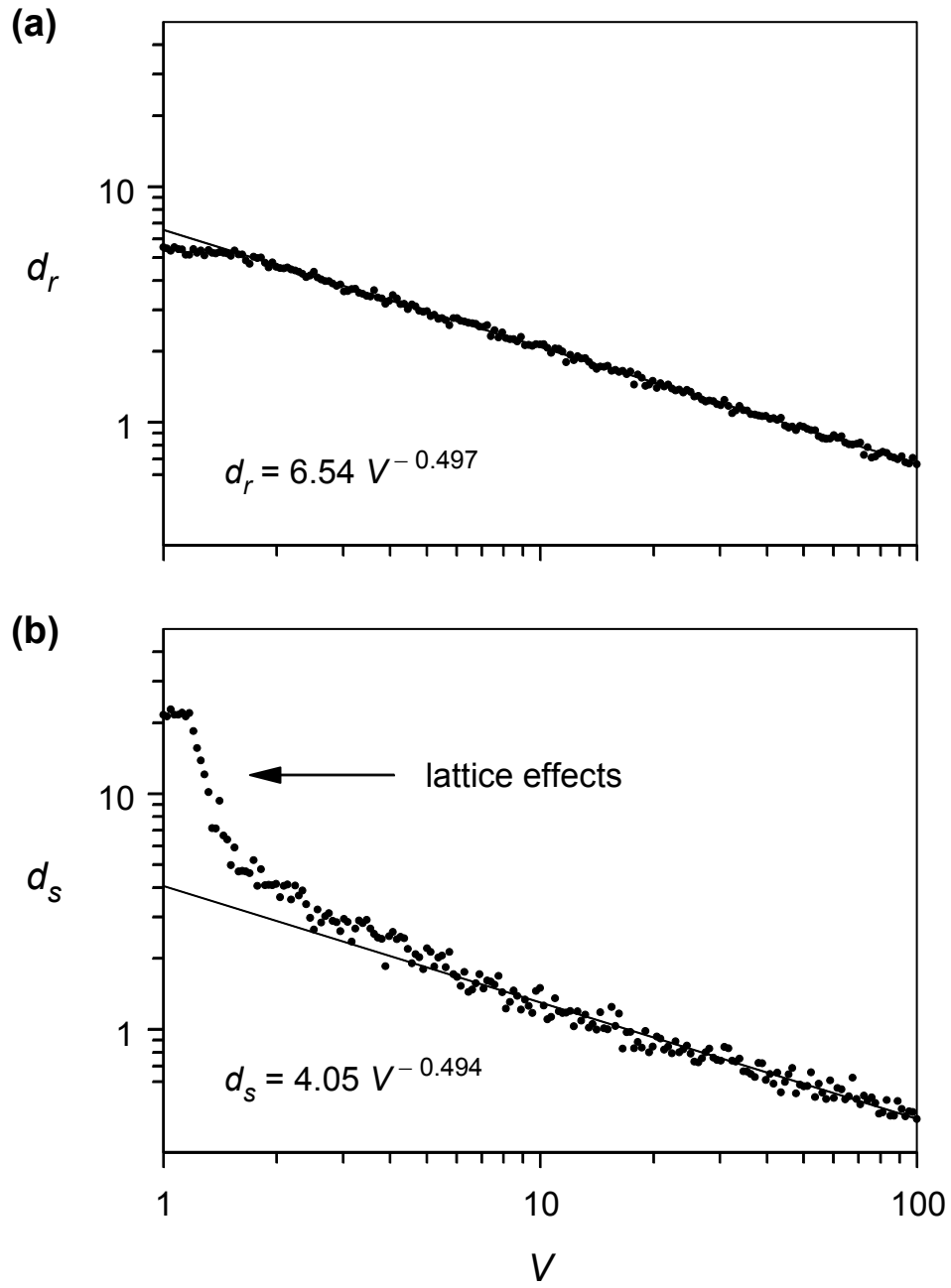


Figure 4

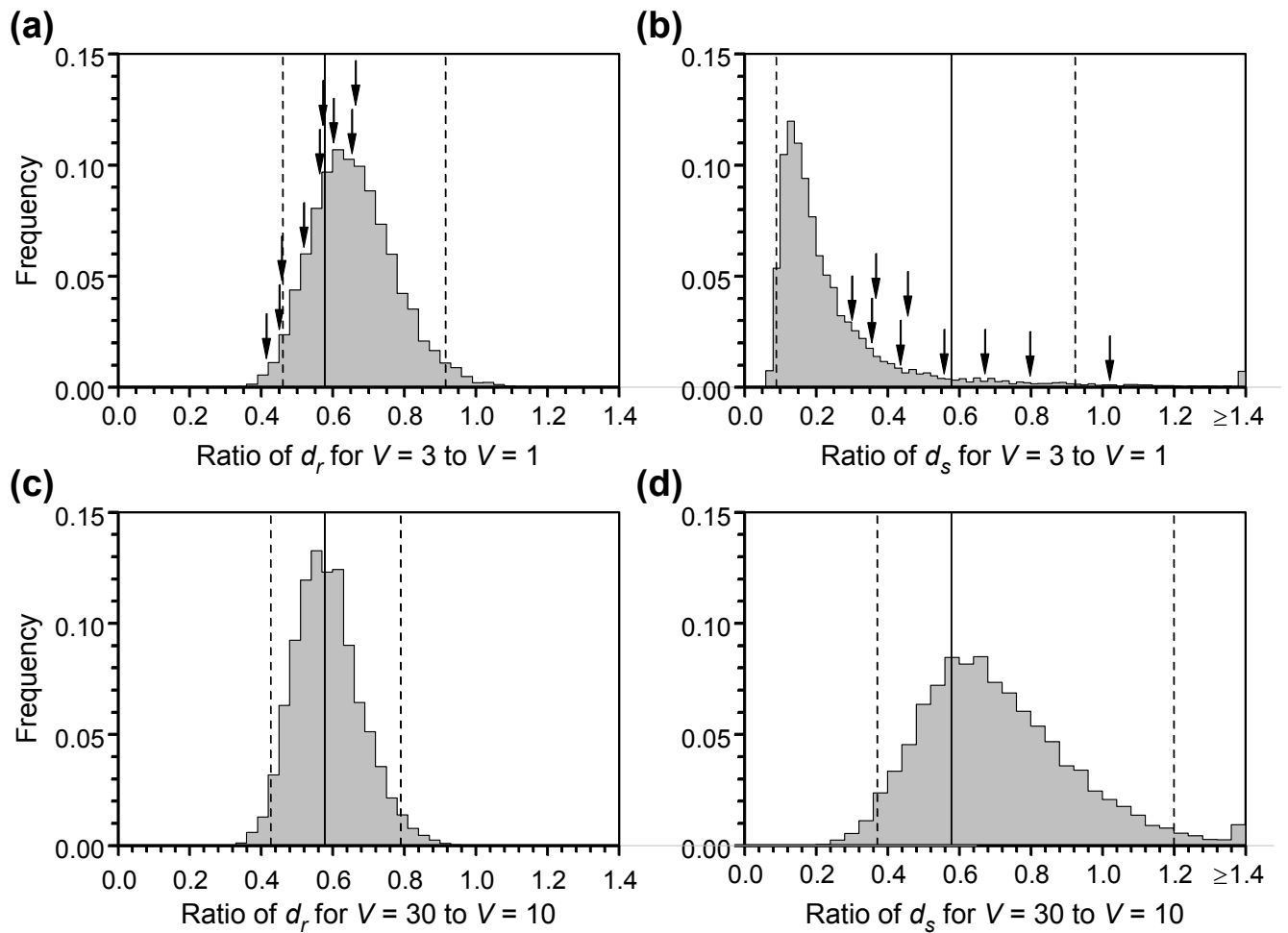


Figure 5

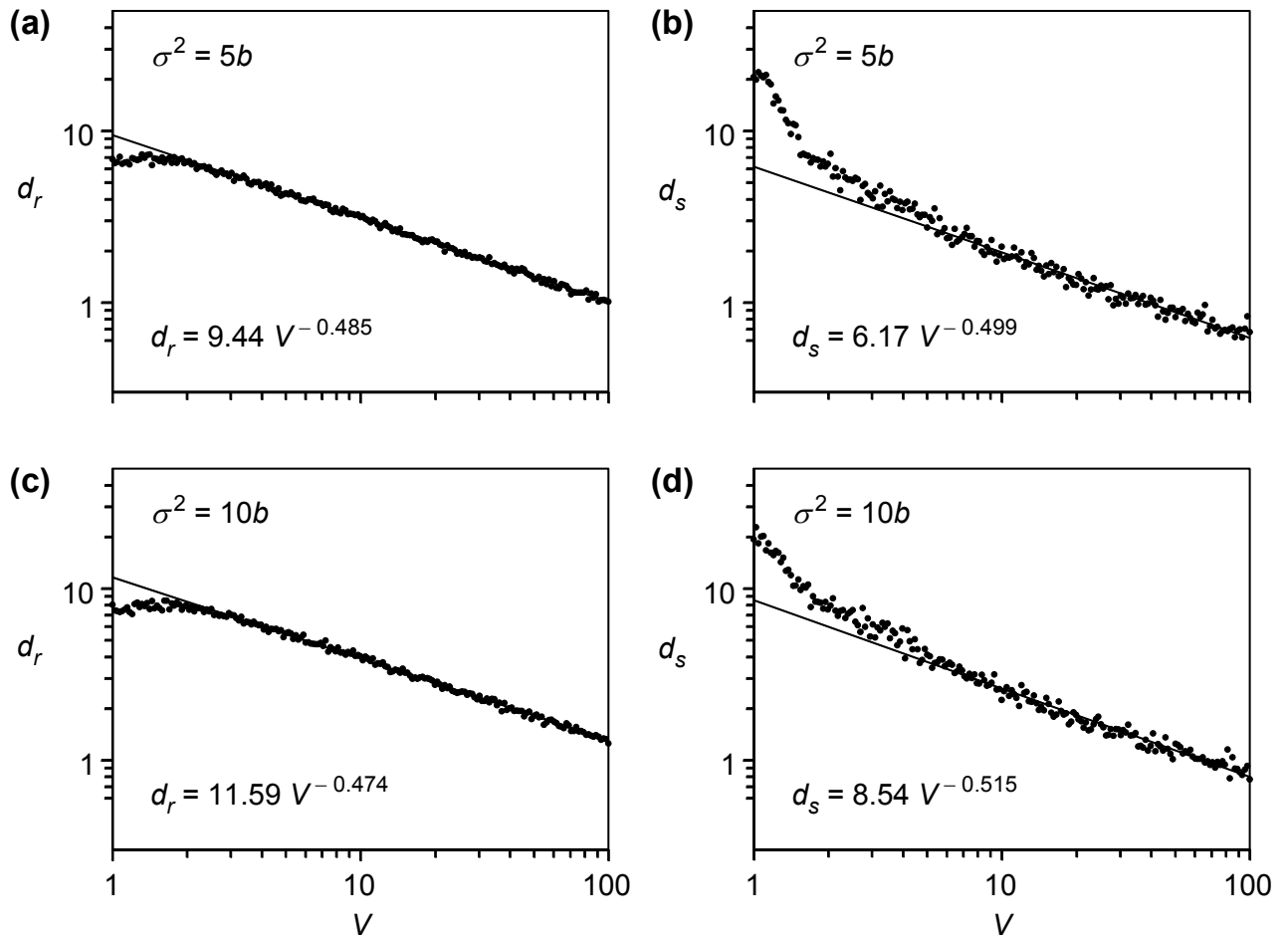


Figure 6